OPTIMIZING THE PROCESSING OF SAPPHIRE WITH ULTRASHORT LASER PULSES

Paper #M403

Geoffrey Lott[1], Nicolas Falletto[1,2], Pierre-Jean Devilder[2], Rainer Kling[3]

[1] Electro Scientific Industries, 13900 NW Science Park Drive, Portland, Oregon, 97206
[2]Eolite Systems, 11 Avenue Canteranne, 33600 Pessac, France
[3]Alphanov, Institut d'Optique d'Aquitaine, 33400 Talence, France

Abstract

The ability to rapidly and precisely generate high-quality features with small dimensions in sapphire is paramount for broadening its appeal and expanding its utilization for consumer electronics applications. Intrinsic properties of sapphire, including high scratch resistance, make it an attractive option for these purposes, but the ability to machine fine features in sapphire substrates with common mechanical and laser-based methods has proved elusive to this point. In this study we present results from a series of systematic trials to determine the optimum laser processing parameters for drilling 400µm diameter holes with no cracks or chips and <5° taper in 430µm thick sapphire wafers with a 0.8 picosecond 1030nm source. Holes are drilled at repetition rates from 21kHz to 1042kHz, overlaps from 70% to 98%, and translation of the beam waist through the sample at rates from 10µm/s to 200µm/s. We present qualitative and quantitative results generated from laser scanning microscopy demonstrating that holes with <5° taper and no cracks or chips can be drilled at repetition rates of 260kHz with 90% and 95% overlap and 521 kHz with 95% overlap. We find that the optimum processing parameters for drilling holes with <5° taper correlates well with the conditions necessary for avoiding chipping, cracking, and back-side damage rings. Holes with <5° taper can be drilled in as short as 4-6 seconds per holes, and holes with <2° taper can be drilled in 10-12 seconds per hole.

Introduction

The outstanding scratch resistance, corrosion resistance, biocompatibility, and thermal stability offered by sapphire makes it an attractive material for numerous current and next-generation technologies [1, 2]. With a Mohs index of 9, sapphire is one of the hardest known materials. The scratch resistance imparted by this hardness, along with good optical transparency from the visible through mid-IR spectrum, has led to the broad utilization of sapphire as cover glasses in consumer electronics and luxury watches, and as windows for military and civilian vehicles.

Sapphire is a prime material for many medical implants and devices because it demonstrates superior biocompatibility and inertness in comparison to metals and polymers. The thermal stability of sapphire is one of the reasons that it is the predominant choice as a substrate for light-emitting diode, along with its strength and electrical insulation capacity. The high corrosion and thermal resistance of sapphire has found use in many harsh chemical and thermal environments.

As a consequence of its widespread use, worldwide sapphire production has steadily increased in recent years [3]. However, the growth of sapphire use in some markets, including consumer electronics, has lagged behind expectations [3]. Part of the reason for this is that the same hardness that is beneficial for many applications also makes sapphire a very difficult material in which to machine fine structures via conventional and laser processing methods. Laser cutting and dicing of sapphire has been performed by many groups [4-9], but small features have been problematic, or have required relatively complex processes [10].

Towards these ends, we have performed laser ablation studies of sapphire using ultrashort pulsed lasers in diverse processing conditions utilizing a standard scanning galvanometer for beam delivery. In the remainder of this paper we will present results for optimizing the quality of drilling small holes (<500µm diameter) in 430µm thick sapphire wafers. We have performed studies with a 0.8ps, 1030nm laser source. The aim of this work is to define the parameter space for drilling holes in terms of repetition rate, pulse overlap, and the z-axis translation speed of a bottom-up ablation process. The goal is provide holes free of chips, cracks, or other damage with average taper angles of <5° and drilling speeds of as low as 5 seconds per hole. These goals are realized throughout these tests. Holes with taper lower than 2° are able to be achieved at slower processing speeds. These results demonstrate the potential for current-generation industrial lasers to generate internal features in sapphire with a small form factors and acceptable throughput by utilizing standard laser micromachining tools.

Experimental

These studies are performed with a 0.8 picosecond 1030nm laser, verified with autocorrelation and a spectrum analyser, with a maximum on-sample pulse energy of 26.4µJ and repetition rate of up to 3MHz. The experimental apparatus uses a scanning galvanometer (20mm entrance aperture) and 100mm telecentric focusing lens. A 4x beam expander increases the 99% beam diameter from 4.6mm to 18mm, generating a measured $1/e^2$ beam waist of 18µm on sample for a peak fluence of 20.7 J/cm^2. Polarization of the laser beam is linear out of the laser, and is changed to circular polarization on-sample by use by use of a λ/4 waveplate.

The pattern for all drilling processes presented herein is a spiral with an added circular revolution at the full spiral diameter for each spiral repetition (inward + outward return path) to optimize quality of the feature edges. A rough sketch of the pattern cross-section is depicted in Figure 1. Processing parameters including scanning speed/overlap, laser repetition rate, and z-axis translation speed are varied throughout these studies in order to determine the optimum processing conditions for sapphire drilling with 0.8ps pulses. Pitch is held constant at 9µm (half the beam waist) for all tests. All tests are conducted with the maximum pulse energy on sample of 26.4µJ. Experiments are performed in ambient air without any gas shielding.

430µm thick, 50.8mm diameter dual-polished c-plane sapphire wafers are used throughout these studies. The effective thickness for machining these wafers – the distance that the beam waist must be translated along the z-axis to move from the top surface of the wafer to the bottom surface (or vice versa) – is ~250µm, equal to the 430µm thickness of the sapphire wafer divided by its index of refraction (n = 1.75).

Holes are drilled by using an ablative process in a bottom-up geometry, as shown in Figure 1. The bottom-up ablation method has been utilized to generate zero-taper holes in a wide variety of transparent media in previous works [11-13]. In this configuration the laser beam begins with its beam waist below the bottom surface of the sapphire wafer. When processing begins, the beam waist is translated upwards (i.e. through the sample) at a constant velocity along the z-axis, with speeds typically between 10µm/s and 50µm/s or higher. Movement along the z-axis ceases when the beam waist reaches the top surface of the sapphire sample. If the hole has not completed drilling at this point, the laser pattern continues to run until the hole is fully drilled. Throughout the drilling process, plasma is visible to the eye. When drilling is complete, the spiral pattern ceases to be visible, and sample processing is immediately stopped manually.

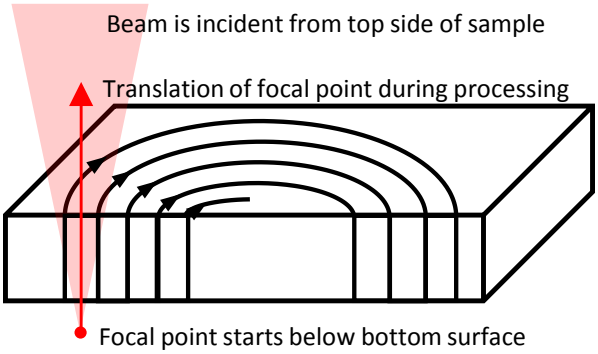

Figure 1: Bottom-up ablation geometry and spiral pattern cross-section.

In Figure 2 we present examples of the highest quality holes that are generated in these tests, and we also present examples of detrimental characteristics that we wish to avoid. In these pictures, the textured area in the middle of the holes is from the sample stage of the laser scanning microscope, and is not indicative of anything positive or negative regarding the quality of the holes drilled in sapphire. The high-quality top and bottom surface images (left panels) demonstrate very low taper (<2°), no/minor chipping, and no cracking. On the top surface, we point out that the galvanometer delays are not perfectly set, and a small lead-in for the spiral is visible, but it does not result in any damage. The bottom surface diameter is nearly identical to that of the top (typically <5µm difference), and also reveals no chipping or cracking. In contrast, the images from poor quality holes in the right panels indicate larger taper (>9°), significant cracking, and multiple back-side damage rings. We note that the image for the poor-quality bottom surface hole is at a lower magnification than the other three images in Figure 2 in order to better capture the damage ring. The formation of these damage rings has previously been ascribed to a filamentation effect on the curved edges of transparent material during processing. In the scope of this paper we will not examine these damage rings further, we will only focus on determining processing conditions that avoid their creation.

Though we observe the hole diameter on top and bottom surfaces to be nearly identical, we do not observe the generation of zero-taper holes in any experimental conditions. The reason for this is the redeposition of molten sapphire particulates along the hole sidewall during processing. This is visible in both the high-

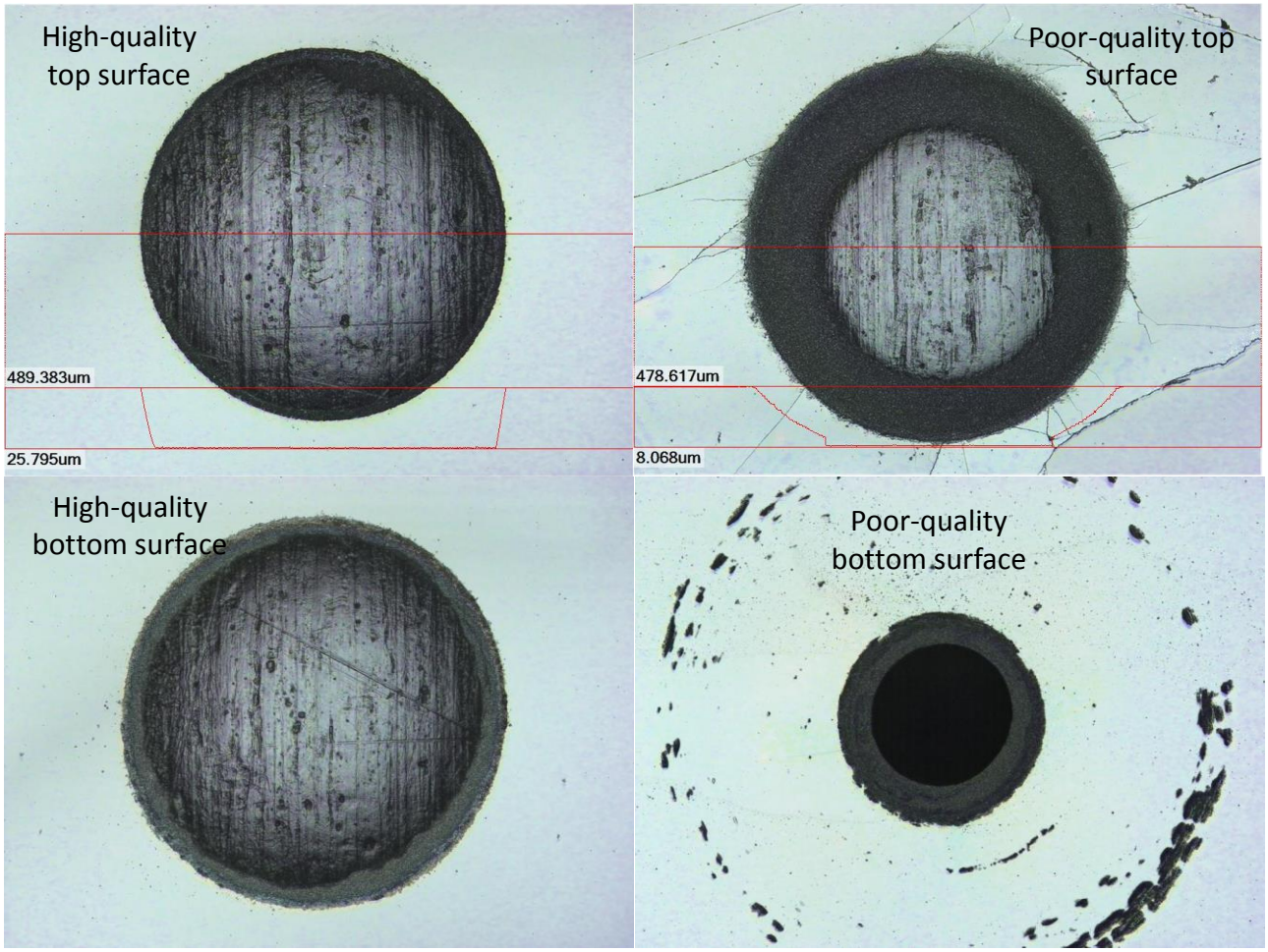

Figure 2: Examples of top and bottom for excellent quality holes (left) and poor quality holes (right).

quality and poor-quality results in Figure 2 – in both cases, dense aggregates of molten sapphire particulates are observed inside the hole on the bottom side of the sapphire wafer (i.e. the side that the ablated material must be ejected from during bottom-up processing). In this paper we will determine the parameters that yield the lowest taper, and therefore the least amount of redeposited material along the hole sidewall. Processed samples are gently cleaned with an alcohol swab to remove debris and particulates from the wafer surface, but no attempts are made to remove redeposited material from the inner wall of the holes. Future studies will examine techniques for reducing this redeposition during processing, and for removing the redeposited material with post-processing.

The profiles of holes generated with these processes are analysed with a laser scanning microscope (Keyence VK-9700, VK9710) to determine quantitative parameters such as maximum (i.e. hole entrance) and minimum hole diameter and average taper angle, as well as qualitative characteristics including cracking and chipping. Images are generated with 2µm step size across the entire thickness of the sapphire wafer. Each hole is analysed across two orthogonal lines, and the results for hole entrance diameter and internal hole diameter are averaged for these two lines. These results are used to determine the hole taper angle. The average taper angle, θ, of each hole is determined from the hole diameter on the top surface (T), the minimum internal hole diameter (B), and the sample thickness (h):

$$\theta = \tan^{-1}\left(\frac{T-B}{2h}\right) \quad (1)$$

Results and Discussion

Drilling holes that are very small in diameter and high in aspect ratio (sample thickness : hole diameter) often results in an extremely restricted parameter space for generating high quality holes, from which little useful general information can be learned. On the other hand, drilling holes that have a large diameter and low aspect

ratio results in a very broad effective parameter space that also results in little general information. Trials in this paper are performed with a pattern diameter of 400µm diameter (aspect ratio of ~1), which is expected to be a suitable mid-point between these limiting cases. Therefore, we expect that lessons learned through these studies will be useful as guidelines for helping to determine optimum laser machining parameters for holes from very small (down to 100µm diameter or smaller) to very large (multiple millimeters) dimensions.

400µm diameter holes are drilled with pulse repetition rates of 21kHz, 104kHz, 260kHz, 521kHz, and 1042kHz. At each repetition rate, holes are drilled with overlaps of 70%, 80%, 90%, 95%, and 98% of the beam diameter if possible. As repetition rate is increased, the scanning speed required for any particular overlap must also increase. While the straight line speed of the galvanometer is reliable at speeds of >10m/s, it is important to note that processing speeds for features of 400µm size are restricted to much lower values. We observe that the movement speed is limited to a maximum of <800mm/s for the 400µm diameter spiral pattern. Due to this limitation, we are unable to perform studies on all overlap conditions at all repetition rates.

At each overlap the translation of the focus along the z-axis is varied from 10µm/s to ≥50µm/s, unless significant and regular damage is observed at lower processing speeds. We limit the slowest z-axis translation speed to 10µm/s to ensure that hole throughput remains reasonable. We will present no results for tests performed at 21kHz – holes drilled at 21kHz are occasionally of acceptable quality, but the results are not consistent, and most often result in severe

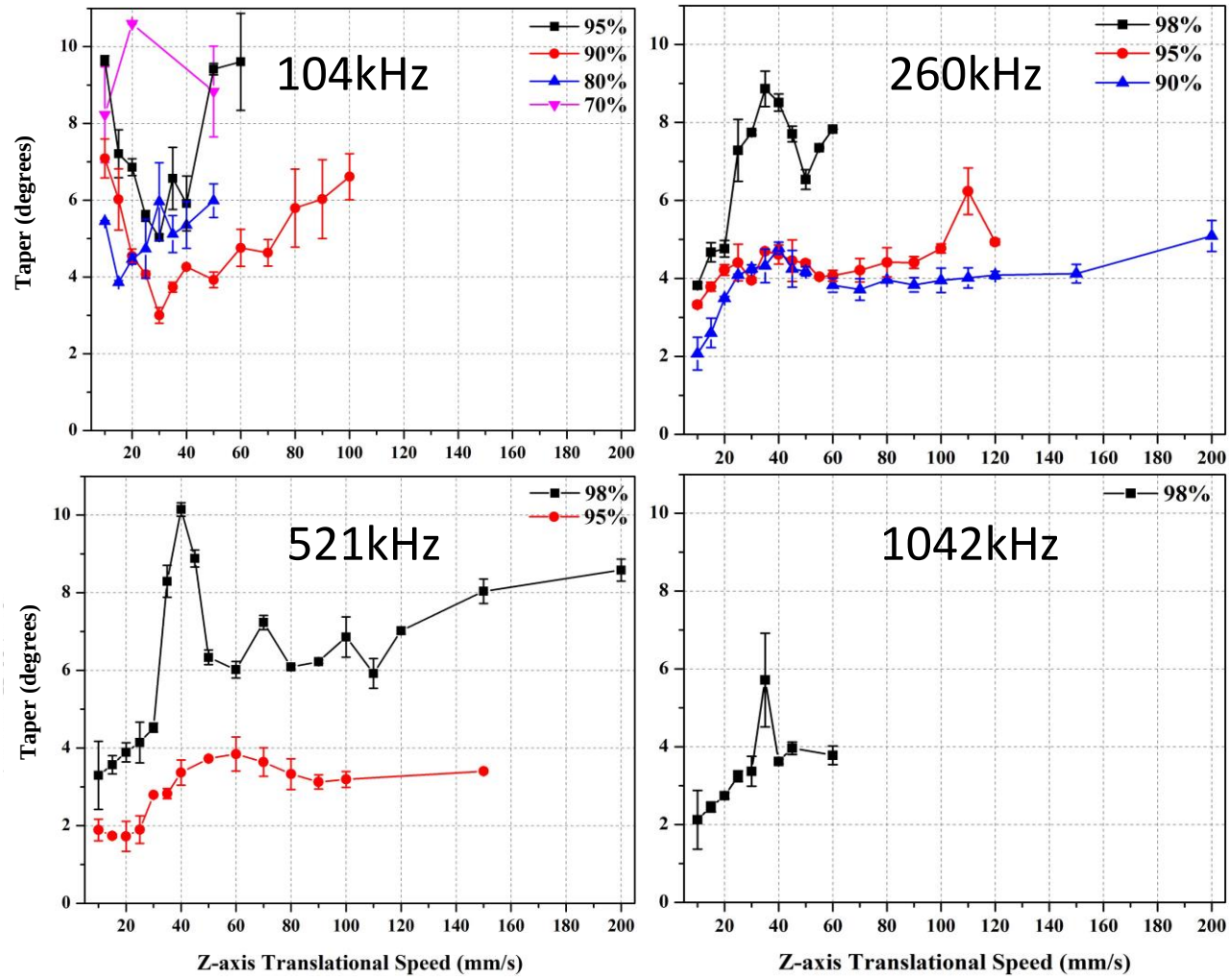

Figure 3: Average taper vs. z-axis translation speed for 400µm diameter holes drilled with repetition rates of 104kHz (top left), 260kHz (top right), 521kHz (bottom left), and 1042kHz (bottom right). Separate lines are shown for each individual overlap condition.

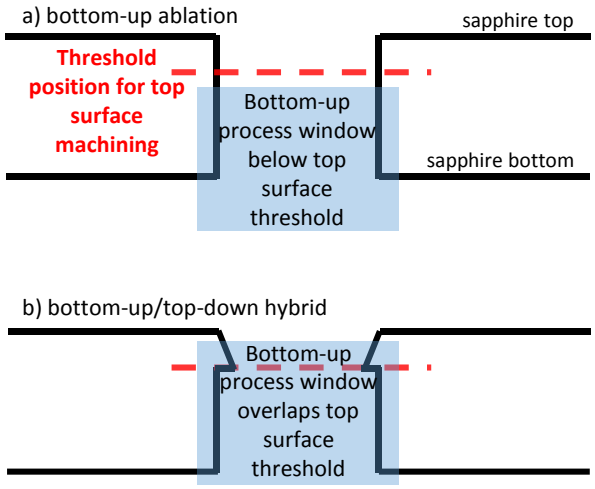

Figure 4: Diagram of conditions necessary for drilling holes (a) entirely with bottom-up ablation, and (b) hybrid bottom-up/top-down ablation.

cracking and damage to the sapphire substrate across all z-axis translation speeds and overlaps.

Minimizing Taper

Taper values calculated using Equation 1 for this array of repetition rates, overlaps, and z-axis speeds are shown in Figure 3. Error bars are determined from differences in taper calculated from the two orthogonal hole profiles, as described above.

Let us first consider results generated at 260kHz with 90% overlap (top right, blue data). As a function of z-axis translation speed, it appears that the evolution of the taper can be separated into two distinct regions – an approximately linear regime at high speed (≥60µm/s) and a more complex regime at speeds <60µm/s. In this lower speed range, we see an increase in taper as the z-axis translation speed is increased from 10µm/s to 40µm/s, and then a slight decrease in taper as the speed is increased from 40µm/s to 60µm/s. For this data set, the value of 40µm/s corresponds to the highest z-axis translation speed that, observed by eye, drilled a hole with only bottom-up ablation and not a hybrid bottom-up/top-down process. At low z-axis translation speeds (≤40µm/s in this data set), we observe that the bottom-up process begins with the beam waist far below the bottom surface of the wafer due to heat accumulation and incubation effects [14-16]. These effects are maintained throughout the entire process, and drilling is completed after ~250µm of z-axis translation, before accumulation/incubation effects exceed threshold and initiate ablation on the top surface, as is shown in Figure 4a. However, as the z-axis speed is increased we observe the onset of bottom-up ablation to occur with the beam waist closer and closer to the bottom surface of the sapphire wafer. Consequently, the z-axis value for the end of the 250µm bottom-up processing window also shifts to a higher value. Eventually this process window overlaps the z-axis position that initiates ablation on the top surface of the sapphire wafer. At this speed and higher, the process becomes a hybrid bottom-up/top-down process, as shown in Figure 4b.

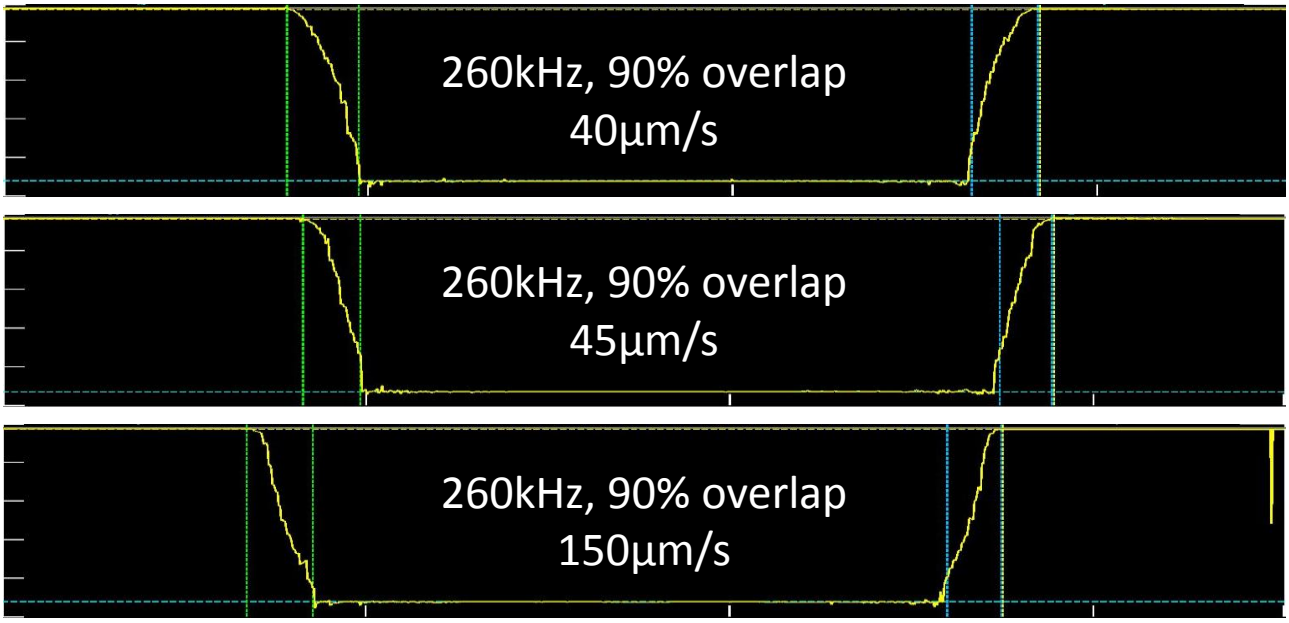

Figure 5: Hole profiles determined by laser scanning microscopy at z-axis translation speeds just below (top), just above (middle), and far above (bottom) the speed observed to transition from a bottom-up ablation process to a hybrid bottom-up/top-down ablation process for holes drilled at 260kHz and 90% overlap.

At slower z-axis speeds that result in this hybrid process, the bottom-up portion of the process proceeds deep into the wafer before switching to the top-down portion of the process. The decrease in taper from 40µm/s to 60µm/s can be understood as follows: since the bottom-up process does not proceed all the way through the wafer, a thin layer of molten sapphire is redeposited along the sidewall. The top-down process creates a tapered wall that does not extend past the thickness of this redeposited layer, resulting in a lower taper than the bottom-up holes generated at the highest speeds before this transition. As the speed is increased beyond 60µm/s, the switch from bottom-up to top-down occurs earlier, resulting in wall taper that does extend past the redeposition layer, resulting in a ledge or overhang that decreases the minimum diameter of the hole and therefore leading to the general trend of increasing taper from 60µm/s to 200µm/s.

This transition from a solely bottom-up process to a hybrid process is also confirmed by the curvature of the hole wall as determined by profilometry measurements. The bottom-up process generates walls that are slightly convex towards the top surface of the sapphire wafer, while hybrid holes that are completed with the top-down process are concave, as is characteristic in general of a top-down process. This can be observed in Figure 5 – the difference in sidewall curvature from 40µm/s to 45µm/s in this data set at 260kHz and 90% overlap is subtle, but visible. The effect becomes more pronounced as the z-axis translation speed is further increased, as shown in the bottom panel of Figure 5 for 150µm/s.

As the overlap is increased to 95% at 260kHz, the observations and trends that we have characterized for 90% overlap at 260kHz are in excellent agreement, albeit with slightly higher average taper values at 95% than at 90%. Similarly, these observations can be extended to overlap of 98%, though the holes begin to exhibit serious, large cracks at 30µm/s and higher, so the data set was truncated at 60µm/s. The pattern speeds required for overlaps of 80% and 70% at 260kHz are above 800mm/s, and are therefore too high for the galvanometer to maintain at this pattern size..

We have now observed that the average taper angle for holes drilled at 260kHz increases as overlap is increased, and as the z-axis translation speed is increased. Both of these trends correspond to increased taper when the spatial periodicity of the spiral pattern along the z-axis is increased – when the spiral pattern speed is decreased (i.e. overlap is increased), the distance between successive patterns repetitions along the z-axis is also increased, which is also true when the process speed along the z-axis is directly increased. We speculate that this may also contribute to the observed increases in average taper angle, but have not yet examined cross-sections of drilled holes as a function of these variables to confirm or refute this speculation.

These trends as a function of z-axis translation speed at 260kHz also apply to results at 521kHz and 1042kHz, though there are fewer accessible overlap conditions at higher repetition rates, and the 98% overlap data set at 1042kHz is not continued past 60µm/s due to considerable cracking and surface damage. At higher repetition rates, incubation effects are increased, shifting the beginning of the bottom-up processing window below that of a lower repetition rate at the same overlap and z-axis translation speed. This results in onset of the hybrid process at a higher z-axis translation speed at higher repetition rate. This is clearly visible at 95% overlap for 521kHz, where the transition was observed by eye to occur at 50µm/s instead of 40µm/s as for 260kHz. It is difficult to confirm this behaviour for 98% overlap at 521kHz and 1042kHz due to larger fluctuations in taper and significant damage to most holes drilled in these conditions. Series of holes drilled at 104kHz deviate strongly from trends at higher repetition rates for all overlaps studied. These holes are of relatively poor quality and exhibit a very high likelihood of cracking. We will examine the reasons for this in more depth in the following section.

An important consequence of this hybrid process to consider is the effect that it has on throughput. When the process is comprised solely of bottom-up ablation, the drilling time for a single hole is equal to the effective sample thickness of 250µm divided by the z-axis translation speed. The hole taper is generally minimized at the slowest z-axis translation speeds, with the obvious drawback of low throughput in these conditions. For speeds of 40-50µm/s, which is towards the limit for bottom-up-only processing, this equates to a drilling time of 5-6 seconds per hole. When the hybrid process begins to occur, the process time ceases to be inversely proportional to the z-axis translation speed, and we observe the process time to fall in the 5-10 second range. Therefore, since there are no improvements to throughput and minimal potential reductions in hole taper, we conclude that there are no significant advantages to z-axis translation speeds at or above the level that causes the hybrid bottom-up/top-down process to occur. Holes with sidewall taper of <5 degrees can be generated with a wide range of z-axis speeds at 260kHz (90% and 95% overlap) and 521kHz (95% overlap).

In many applications, a straightforward way to increase throughput is to increase the repetition rate – for example doubling the repetition rate to apply double the

average power is expected to increase throughput by a factor of two in many instances [14]. These results do not follow that expectation. For example, the galvanometer movement speed for 90% overlap at 260kHz is identical to that for 95% overlap at 521kHz, but the potential throughput only increases a small amount, as described in the previous paragraph, due to a shift in the process window for bottom-up ablation due to enhancements of thermal accumulation and incubation effects.

In summary, holes with sidewall taper <5° can be generated with a wide range of z-axis speeds at 260kHz (90% and 95% overlap) and 521kHz (95% overlap). The fastest process, near the transition from a bottom-up process to a hybrid process, generates holes with 4-5° taper in 5-6 seconds. If lower taper is desired, it can be

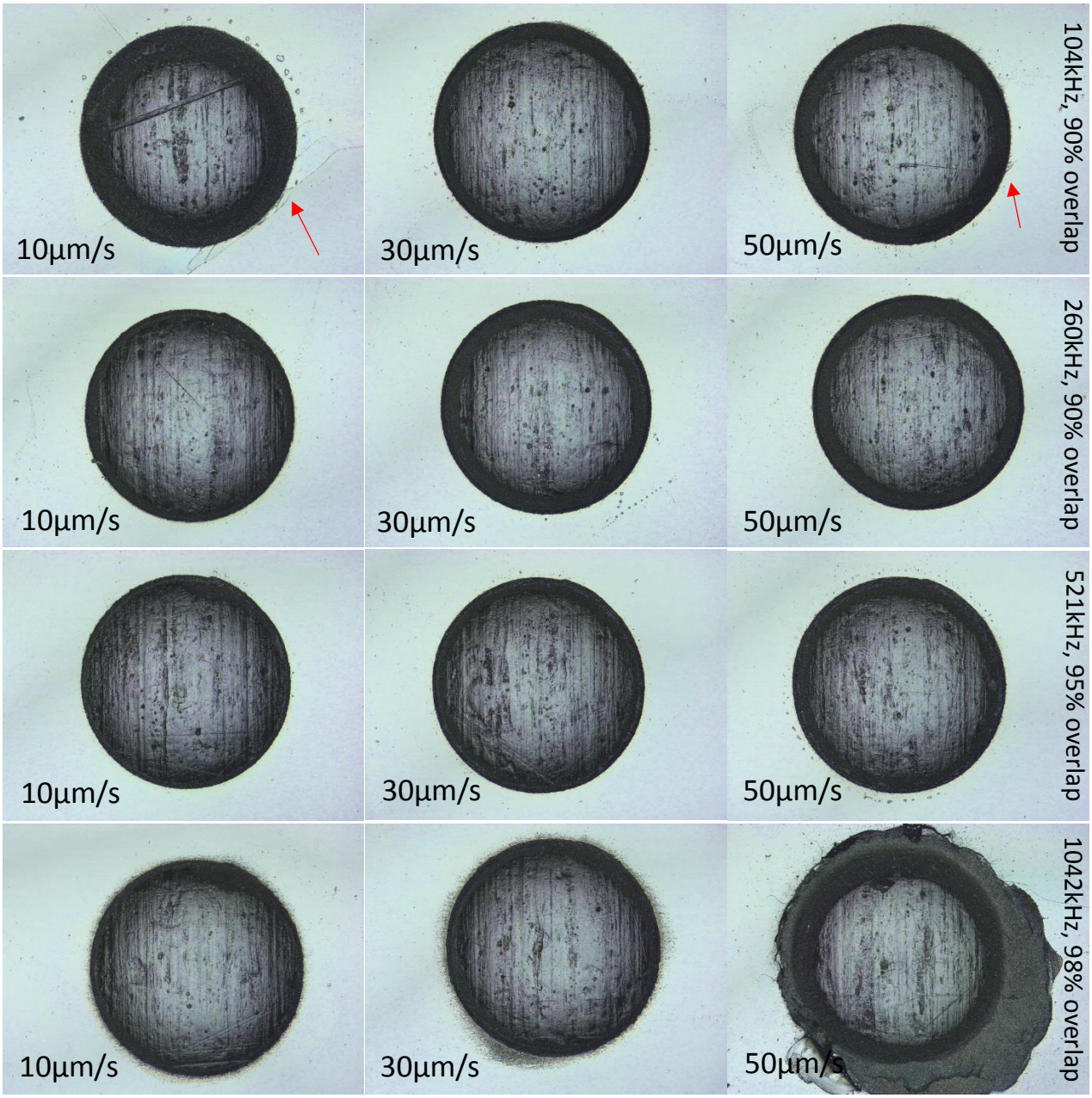

Figure 6: Laser scanning microscopy pictures of top surface of 400µm diameter holes drilled with repetition rates of 104kHz (top row), 260kHz (second row), 521kHz (third row) and 1042kHz (bottom row). Pictures shown are representative of the evolution of hole quality as a function of z-axis/processing speed. Red arrows on 104kHz pictures are placed to guide the eye to cracks/damage.

achieved at the expense of throughput, with average taper values observed below 2° near 20µm/s at 521kHz.

Avoiding Cracks and Chips

Now that we have defined conditions for generating low taper holes in sapphire with acceptable throughput, we must consider the quality of the holes beyond taper: what conditions are necessary to avoid cracking and chipping during processing, and how does this affect the process window that was determined while only considering taper and throughput?

We present representative pictures of hole quality at different z-axis speeds and repetition rates in Figure 6. At each repetition rate, the overlap is chosen that demonstrated the best hole quality and least amount of cracking. The circularity and symmetry of all holes is excellent and is consistent across the entire parameter space that is tested. In the top row, holes generated at 104kHz and 90% overlap are shown. At 10µm/s, the hole shows large taper (7°, as per Figure 3) and cracking. Holes drilled at 30µm/s and 50µm/s each have less taper, though the hole at 50µm/s is cracked. The holes at 260kHz (90% overlap) and 521kHz (95% overlap) in the second and third rows of Figure 6 progress similarly – both increase slightly in taper from 10µm/s to 50µm/s (from ~2° to ~4°), and no holes in this z-axis speed range are cracked. Holes at 1042kHz (bottom row) proceed similarly to those at 260kHz and 521kHz in terms of taper, but the quality is clearly decreased – very severe damage is evident at 50µm/s, and sticky particulates are visible at 10µm/s and 30µm/s. Similar particulates were easily removed from holes generated at lower repetition rates with a gentle alcohol swab, but remained partially on the surface at 1042kHz. This reflects increased thermal effects while processing at high overlap and high repetition rate.

In Figure 7 we present a plot of hole quality vs. taper, where we assign a value of "1" to holes with no cracking and (at the most) very minor chipping, and a value of "0" to holes with visible cracks and/or chips. Results from all holes generated at repetition rates of 104kHz, 260kHz, 521kHz, and 1042kHz are compiled in this plot. We observe a clear demarcation in the likelihood of hole cracking for taper values below and above 5°. For holes with taper of ≤5°, we find no chipping or cracking 86% of the time. For holes with taper >5°, however, no chipping or cracking was only observed in 24% of cases. This demonstrates a strong correlation between hole quality and taper. Overall, this agrees well with the process window defined in the previous section – holes drilled in sapphire with low taper (≤5°) are unlikely crack or exhibit large chipping. With the large parameter space explored in these experiments, parameters for individual holes are not generally tested more than once or twice, which could easily result in false negatives or positives in terms of hole cracking. Figure 7 suggests that working with parameters that generate holes with lower than 5° taper ensures a high likelihood of successful drilling. The best conditions for avoiding cracks are therefore 260kHz at 90% and 95% overlap, and 521kHz at 95% overlap. Tapers for all three of these sets of conditions remain below 5° at z-axis movement speeds through the transition from bottom-up ablation to the hybrid process.

In addition to cracking and chipping, we must also consider the conditions that result in the formation of back-side damage rings during processing. The magnitude of these damage rings can vary strongly, as

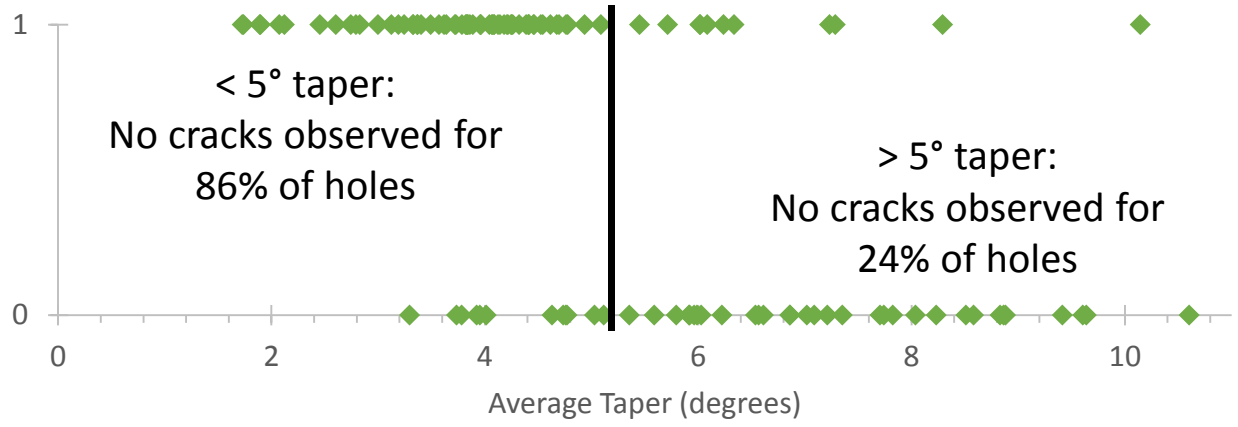

Figure 7: : Hole quality vs. taper angle for all holes drilled at repetition rates of 104kHz, 260kHz, 521kHz, and 1042kHz. Holes are attributed a value of "1" if they do not have cracks or significant chips, and a value of "0" if there is significant chipping or any cracking.

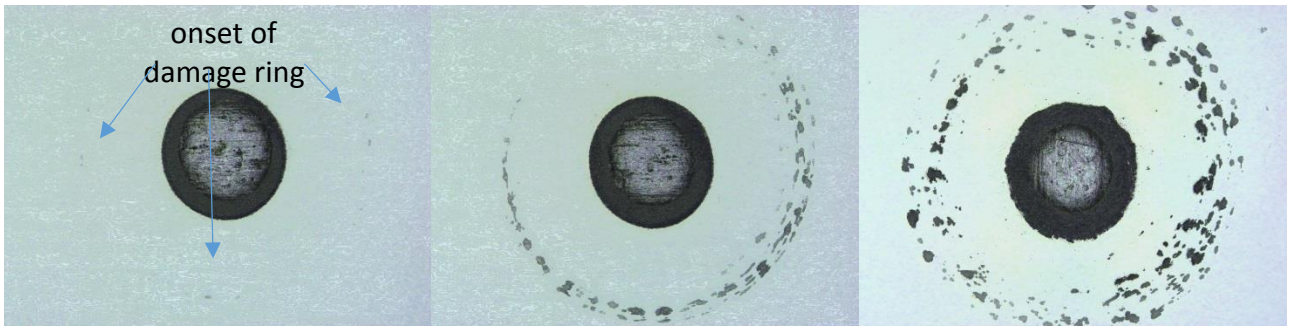

Figure 8: Evolution of back-side damage rings from minor, barely visible effects (left) to very prominent damage that also results in decreased back-side hole quality.

shown in Figure 8. Here, we present examples of a damage ring that has just barely started to form (left panel) and could easily be missed if one were not specifically looking for it, along with much more obvious damage rings (center and right panels). When these damage rings are most readily apparent, they can also affect the edge quality of the hole at the bottom surface, as in the rightmost example. In brief, trends for the appearance of these rings are not as clear as those for cracks and chips. As with cracking, the presence of damage rings is strongly linked to large taper angles, and the acceptable process parameter space is comprised of 260kHz at 90% and 95% overlap, and 521kHz at 95% overlap. As mentioned above, similar damage has been reported in glass drilling processes and has been attributed to filaments created at the top edge of the hole that propagate all way through the substrate before creating damage at the bottom surface.

Conclusions

Promising sapphire drilling results for 400µm diameter holes have been achieved with a fiber laser system of 0.8ps pulse duration. The process initialisation due to nonlinear absorption and the control of the dynamic interplay of energy deposition, material ejection and heat dissipation in the substrate define a process window at fairly high repetition rates (typically 500kHz) and high pulse overlap (90-95%) to maintain the bottom-up process for the entire drilling process. Under these conditions drilling of 400µm holes in 430µm substrates could be obtained within less than 5s with a taper angle below 5°. Holes with a taper angle below 2° could be completed in less than 12s.

At a certain point during the drilling procedure the lifting of the focus position surpasses the threshold of surface absorption. This is the transition point when the bottom-up process switches to the typical top-down ablation mechanism which is affected by larger taper, a higher likelihood of cracking, and poor backside quality. If hole has been completely drilled before this transition point then no top-down process is observed. Therefore the general finding within this study is that process speed and quality both benefit from the bottom-up process. The higher the percentage of the overall process is top-down ablation, then the more pronounced are taper angle, cracking, and back-side damage.

In addition, the poor quality results at low repetition rates when maintaining the other process parameters constant suggest that a fair portion of the deposited energy leads to heat accumulation and preheating of the interaction zone which stabilizes the process due to a smooth temperature gradient profile inside the sapphire sample. Due to its high thermal conductivity the resulting tensile stress profile relaxes as the heat is transported into the bulk which avoids cracking. At low average power the accumulation and thus the preheating of the substrate is less pronounced. In this condition more cracks and chips occur. To support this assumption, diagnostics like temperature profile measurements as well as 3D modelling of heat profiles are necessary, which we intend to carry out in future trials. Furthermore, we will extend the knowledge gained throughout these studies towards the laser machining of high quality holes with low taper at dimensions both smaller and larger than 400µm in diameter.

REFERENCES

[1] Dobrovinskaya, E.R., Lytvynov, & L.A., Pishchik, V. (2009) Sapphire: Material, Manufacturing, Applications, Springer, 481pp.

[2] Virey, E. (2015) Does the US$620M new sapphire related investment at Lens Technology signals the rebirth of the sapphire industry?, www.i-micronews.com

[3] Wang, F. (2015) LEDinside: Sapphire Substrate Market Growth to Soar in 2015, www.ledinside.com

[4] Ashkenasi, D., Rosenfeld, A., Varel, H., Wahmer, M., & Campbell, E.E.B. (1997) Laser processing of sapphire with picosecond and sub-picosecond pulses, Applied Surface Science 120, 65-80.

[5] Baier, T. (2014) High-throughput laser processing of sapphire and chemically strengthened glass, AKL – International Laser Technology Conference, Aachen, Germany.

[6] Gu, E., Jeon, C.W., Choi, H.W., Rice, G., Dawson, M.D., Illy, E.k., & Knowles, M.R.H. (2004) Micromachining and dicing of sapphire, gallium nitride, and micro LED devices with UV copper vapour laser, Thin Solid Films 453-454, 462-466.

[7] Okamoto, Y., Takekuni, T., & Okada, A. (2014) Formation of internal modified line with high aspect ratio in sapphire by sub-nanosecond pulsed fiber laser. Journal of Laser Micro/Nanoengineering 9, 52-58.

[8] Ruettimann, C., Dury, N., Woratz, C., & Woessner, S. (2013) Sapphire cutting with pulsed fiber lasers, ICALEO, Orlando, USA, M403.

[9] Qi, L., Namba, Y., Nishii, K., & Aoki, H. (2009) Femtosecond laser ablation of sapphire, ASPE 24th Annual Meeting, Monterey, USA.

[10] Zibner, F., Fornaroli, C., Ryll, J., He, C., Holtkamp, J., & Gillner, A. (2014), Ultra-high precision helical laser cutting of sapphire, ICALEO, San Diego, USA, M301.

[11] Du, K. (2009) Ready to work: solid state slab laser, Laser Journal 1, 39-43.

[12] Du, K., & Shi, P. (2003) Subsurface precision machining of glass substrates by innovative lasers, Glass Sci. Technol. 76, 95-98.

[13] Karimelahi, S., Abolghasemi, L., & Herman, P.R. (2014) Rapid micromachining of high aspect ratio holes in fused silica glass by high repetition rate picosecond laser, Applied Physics A 114, 91-111.

[14] Di Niso, F., Gaudiuso, C., Sibillano, T., Mezzapesa, F.P., Ancona, A., & Lugara, P.M. (2013) Influence of the repetition rate and pulse duration on the incubation effect in multiple-shots ultrafast laser ablation of steel, Physics Procedia 41, 698-707.

[15] Cheng, J., Liu, C-S., Shang, S., Liu, D., Perrie, W., Dearden, G., & Watkins, K. (2013) A review of ultrafast laser materials micromachining, Optics & Laser Technology 46, 88-102.

[16] Sun, M., Eppelt, U., Russ, S., Harmann, C., Siebert, C., Zhu, J., & Schulz, W. (2013) Numerical analysis of laser ablation and damage in glass with multiple picosecond laser pulses, Optics Express 21, 7858-7867.

Meet the authors:

Geoffrey Lott is an applications engineer for the Laser Business Division of ESI. Previously, he worked at Boise Technology, Inc. for over 4 years as a senior scientist. He earned his Ph.D. from the University of Oregon in 2010. He has expertise in laser micromachining and nonlinear ultrafast vibrational & electronic spectroscopy, and has over 12 years of experience with diverse ultrafast laser systems and technologies. He is an author of several scientific papers and conference presentations.

Nicolas Falletto is application manager for the Laser Business Division of ESI. He is based in the US since 2014. He previously worked for Eolite Systems, France for almost 4 years as an application engineer, and for Quantel Lasers, France in various positions from solid state lasers R&D to fiber laser industrialization and application management. He has experience in laser design and micromachining. He earned his Ph.D. from University of Grenoble, France in 1999. He has collaborated on several scientific and technical papers.

Pierre-Jean Devilder is a product line manager at Eolite Systems (Laser Business Division of ESI). Based in Bordeaux, France, he was formerly a technical director at Eolite Systems. He has been working in the laser field since 1990 with excimers, dye lasers, DPSS, and disk lasers for various companies (Sopra, Nanolase, JDSU, Beamind). He occupied numerous technical positions ranging from development engineer to technical director. He earned his Ph.D. from University of Limoges in 1998.

Rainer Kling is business unit manager for micromachining at Alphanov, France since 2011. From 2002-2011 he worked at Laser Center Hannover (LZH), where he headed the Department of Production and Systems Technology. These functions, and his expertise in photovoltaic technologies, micromachining, and processing of CFRP led him to responsibility in various prestigious organizations. He has published over 50 scientific papers and conference presentations.